CMPE167L Sensing and Sensor Technologies Laboratory
Lab 3: Magnetoresistive Sensors

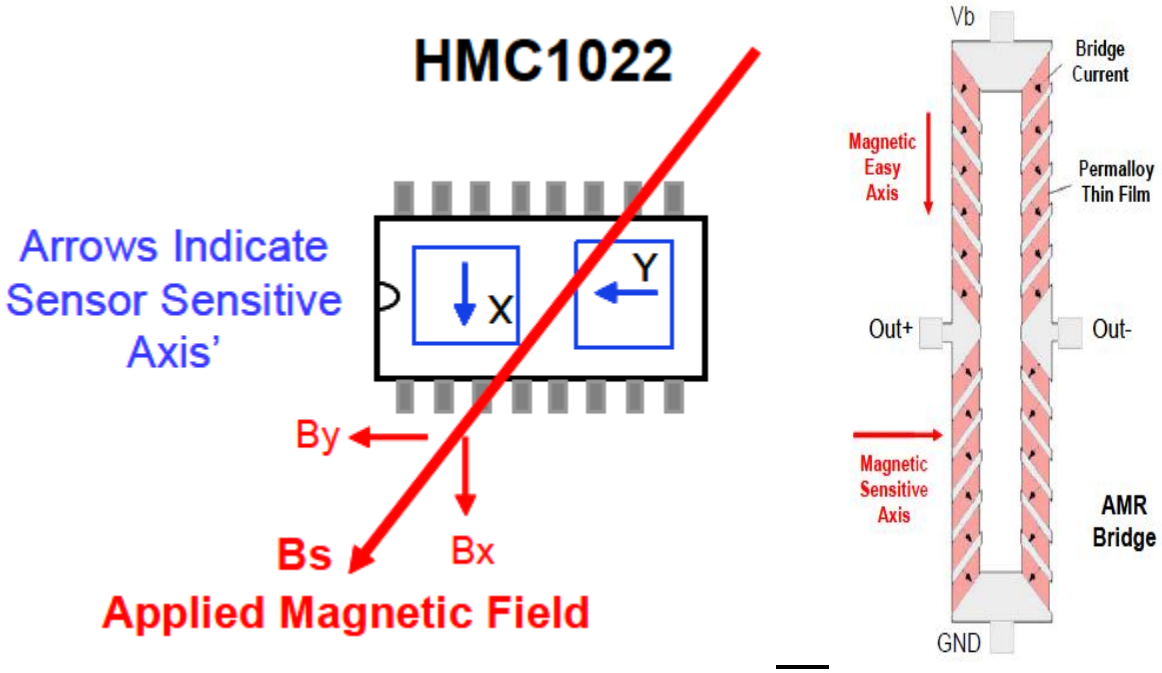

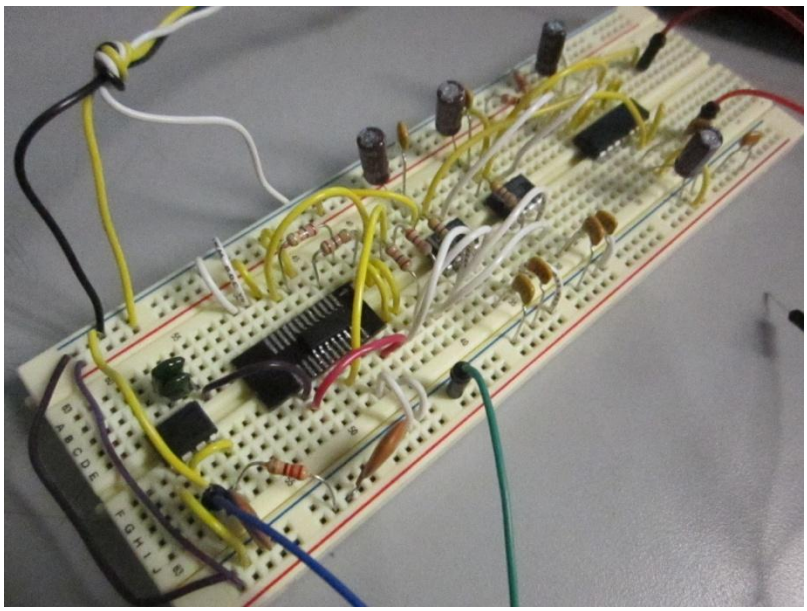

By Troy Pandhumsoporn
Instructor: Stephen Petersen
Date: 5/25/2013
Spring 2013

Introduction:

Magnetoresistive sensors are used in the direct measurement of magnetic fields or magnetic field variation such as magnetic audio recording, credit card reading machines, and magnetically coded price tags. Configured as a four-element Wheatstone bridge, these magnetoresistive sensors convert magnetic fields to a differential output voltage of sensing magnetic fields low magnetic fields. They can also take a more active role in detecting the change of a magnetic field as part of a moving device in the measurements of linear/angular displacements, proximity switches, and position measurement. Unlike similar purposed sensors, magnetoresistive sensors have non-contact operation, robustness to mechanical stress, high sensitivity to weak magnetic fields, vibration-insensitivity (compared to inductors), and usability for elemental hazards (extreme heat/cold). This laboratory explores the use of the Honeywell HMC1022 2-axis magnetoresistive sensor with a system level perspective in measuring the Earth's magnetic field, usually for automotive and hand-held compassing applications.

Experimental Procedures:

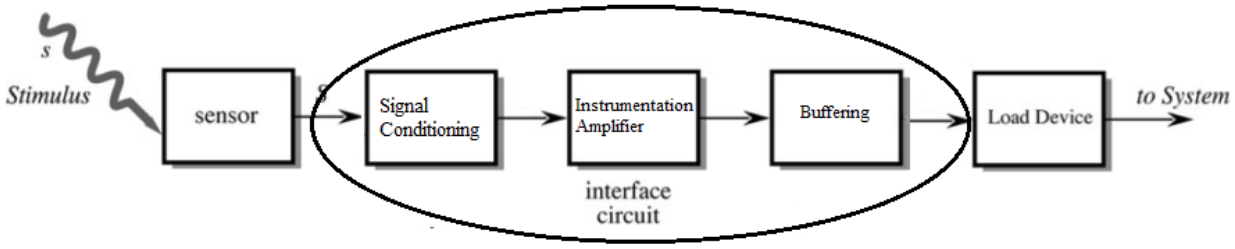

Figure 1: System-level block diagram for general sensor circuits

This modified block diagram from Fraden allows us to classify the circuit into three sections: the HMC1022 magnetoresistive chip as the sensor, the interface circuit consisting of the low-pass filters, instrumentation amplifier, and unity gain voltage buffers, and the load as the NI-6008 DAQ. In the following block diagram, the stimulus is voltage and the system is the LabVIEW GUI and VI setup. The system level perspective that the block diagram provides is instrumental in considering the high-level consequences each block of the system contributes to affecting all the other system components, cascading or compounding inaccuracies through each stage. The ease of intuitively pinpointing the section where errors occur helps simplify and isolate the work engineers have to troubleshoot circuits.

The signal conditioning utilizes one-pole filters that removed the 60 Hz power supply noise from the sensor to the instrumentation amplifier. After observing several common configurations of bridge circuits interfaced to instrumentation amplifiers in Texas Instruments and the Analog Devices handbooks (as well as the midterm exam too), I decided to go along with using instrumentation amplifiers in my implementation. After searching for DIP packages for instrumental amplifiers (an extra $7.00-$8.00 for a SOIC-to-DIP adapter, which is somewhat exceeds/equals the price of the sensor itself), I settled on the LT1167/1168 instrumentation amplifier from Linear Technologies for the characteristics of good power supply rejection ratio (PSSR) and common-mode rejection ratio (CMRR) and easier-to-read datasheet documentation. The AD620 instrumentation amplifier also provides a similar alternative too in cost and package, though I found about that particular amplifier too late after buying the LT1167/1168. The gain

equation that is set by single external resistor is also the same for the LT1167/1168 amplifier as well. With the datasheet sample graphs in mind, I chose the gain resistor of 470 ohms on both instrumentation amplifiers to yield an approximate gain of ~100.

$$G = 1 + \frac{49.4\ k\Omega}{R_G} \cong 106.106$$

Since the bridge output voltage of both magnetometer axes generates 2.5 mV from a 5V bridge supply, the expected output of the instrumentation amplifier should be around 265 mV. Proper high and low frequency bypassing was provided on the power pins of the instrumentation amplifiers for good practice.

<u>Precision Single-Supply Composite In-Amp Output Reference</u>:

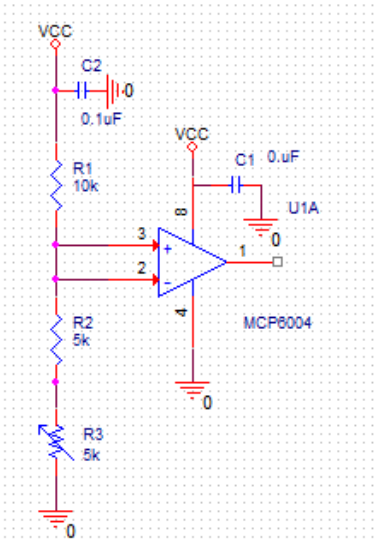

Figure 2: Input circuit to instrumentation amplifier's Vref.

To achieve both high precision and single supply operation of the instrumentation operational amplifier, the designer can use the observation that many popular sensors provide an output signal centered on an approximate mid-point of the supply voltage (or reference amplifier).This basic point permits the inputs of a signal conditioning instrumentation amplifier to be biased at "mid-supply". An instrumentation amplifier referenced to the power supply midpoint followed by a rail to rail op amp output gain stage provides high DC precision. A precision low noise unity gain follower made from the MCP6004 op amp is used to provide low-noise and high DC accuracy. The voltage divider allows us to split the supply voltage in half (+2.5V) with the trimmer for fine adjustment for exactly +2.5V. The voltage divider output is buffered to provide a low-impedance source to drive the reference voltage of the instrumentation operation amplifier. Furthermore, the output voltage is positioned at this halfway mark to allow for bipolar differential input signals. Proper low and high frequency bypassing with a 22/47uF electrolytic and 0.1uF ceramic capacitor can help reduce its noise contribution as well as preserving the resistor ratio using smaller resistors for Johnson noise.

The NI-6008 DAQ was setup with differential inputs with 12-bit resolution (over the 11 bit resolution from single-ended input from the previous lab) and sampled with data at 1000 Hz with analog inputs “ai0, ai1, ai4, and ai5” used.

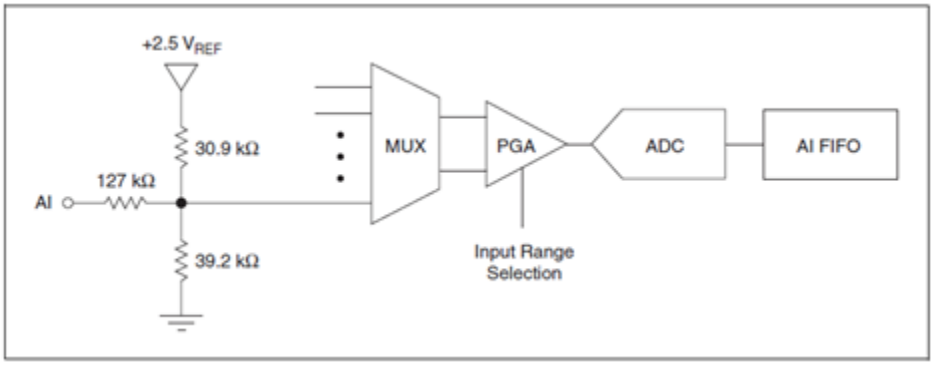

Figure 3: The NI USB-6008/6009 Analog Input Circuitry

Similar to the first laboratory, the impedance looking in through the analog input of the NI DAQ 6008 is 144 kΩ, or 127 kΩ added with the parallel resistance of 30.9kΩ and 39.2 kΩ. Since the designer would want the circuit to have zero impedance from both sides (voltage divider and the DAQ device), simple unity gain buffers are added at the outputs of the instrumentation amplifiers achieves that condition to prevent loading (drawing the low current provided by the DAQ or other devices in Figure 6) and losses by imposing an ideal voltage source fed into the DAQ device.

<u>Set/Reset Straps with P605 chip</u>:

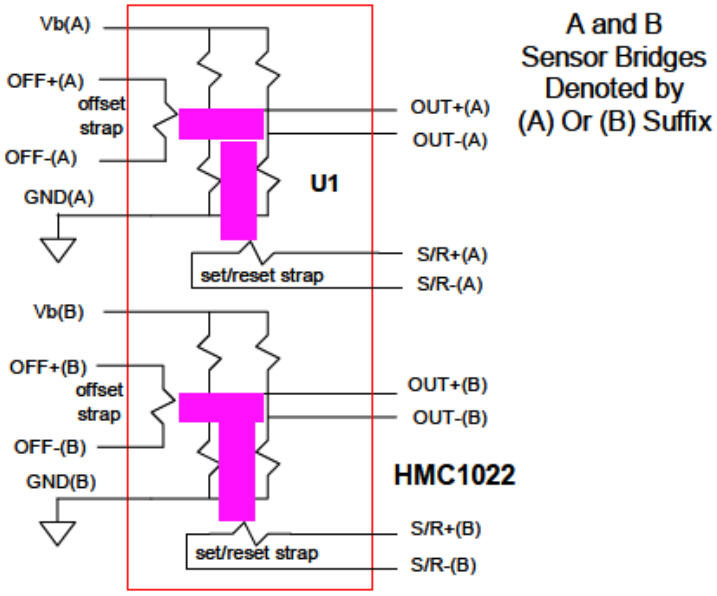

Figure 4: HMC1022 S/R straps pinout

The set/reset straps serve the purpose of sending pulse currents to “degauss” or “de-permalloyize” the sensor bridges as required to avoid sensor performance degradation after exposure to accidental magnetic fields. By periodically sending moderate current pulses at regular intervals, the Permalloy, thin film magnetic domains get re-aligned in the easy axis direction and the memory of the upset field direction is usually erased. The S/R straps reduce the effects of temperature drift, non-linearity errors, and loss of signal output due to the presence of high magnetic fields.

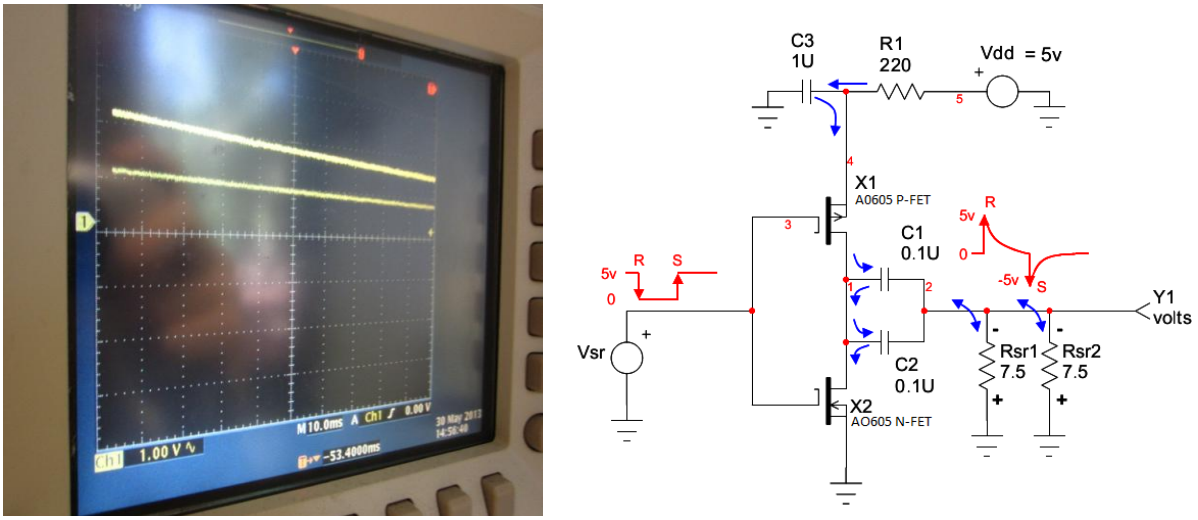

Figure 5: Instantaneous current pulse during set highlight by the upward slant, for the reset, the slant is reversed (negative sloped)

The A0605 Complimentary Enhancement Mode Field Effect Transistor abstracted the totem pole configuration of a P and N-channel power MOSFET on a single PDIP chip as opposed to two separate transistors. Component selection was based on easy-to-find components from the lab kit, with most of the circuit component values followed above schematic for the capacitances; the oscilloscope current pulse would have been shown a lot better if C3 was actually 1 uF instead of the 0.1uF I used to slow down the pulse and pause for the current spikes of switching from ground and power.

The operation of the CMOS totem pole reset (positive pulse) function begins when a input voltage source is held high at Vsr >= 4.5V which turns on the N-channel MOSFET and grounds the parallel capacitances, C1 and C2, and strap resistances, Rsr1 and Rsr2. When the input logic source falls to a lower voltage of Vs <= 0.5 V, the N-channel FET turns off while connecting the strap resistances and the P-FET turns on by pulling on the series RC circuit at the node connecting to the V_{dd} rail. With both parallel capacitances having zero voltage initially, the instantaneous pull-up from ground to the supply rail allows the voltage to flow towards the resistance straps Rsr1 and Rsr2 with voltage drops on the series resistors. As a side note, the designer could have the supply voltage to be a couple volts above the typical 5V to compensate for the voltage drops. While the reset pulse gradually damps out, the series rail capacitor deposits its remaining charge through P-FET to the parallel capacitors C1 and C2 and strap resistances. Sensor measurements can be acquired after the charge accumulation of the capacitances reaches

stability; the result being reverse polarity of the bridge voltage output to the direction of the sensitive axis of the magnetic field input.

For the set (negative) pulse function, both the P-FET and N-FET alternate on and off transitions to close the V_{dd} source through the P-FET and pulling down the connections to parallel capacitors C1 and C2 to ground. This process creates the negative supply voltage across the strap resistances; as a result, it creates a current pulse with a decay rate depending on the on resistance of the N-FET added to the strap resistances and parallel capacitances. A single pole single throw switch could be added to the connected gates of the totem pole to view the current pulses through the oscilloscope more easily as opposed to switching a lead wire from power to ground or vice versa.

Data Acquisition:

Since there have been no existing VI's for the magnetoresistive sensor done before, the VI is crafted to be very simple, with just the DAQ assistant connected to a waveform chart/graph, which is further connected to a Write-to-Measurement block.

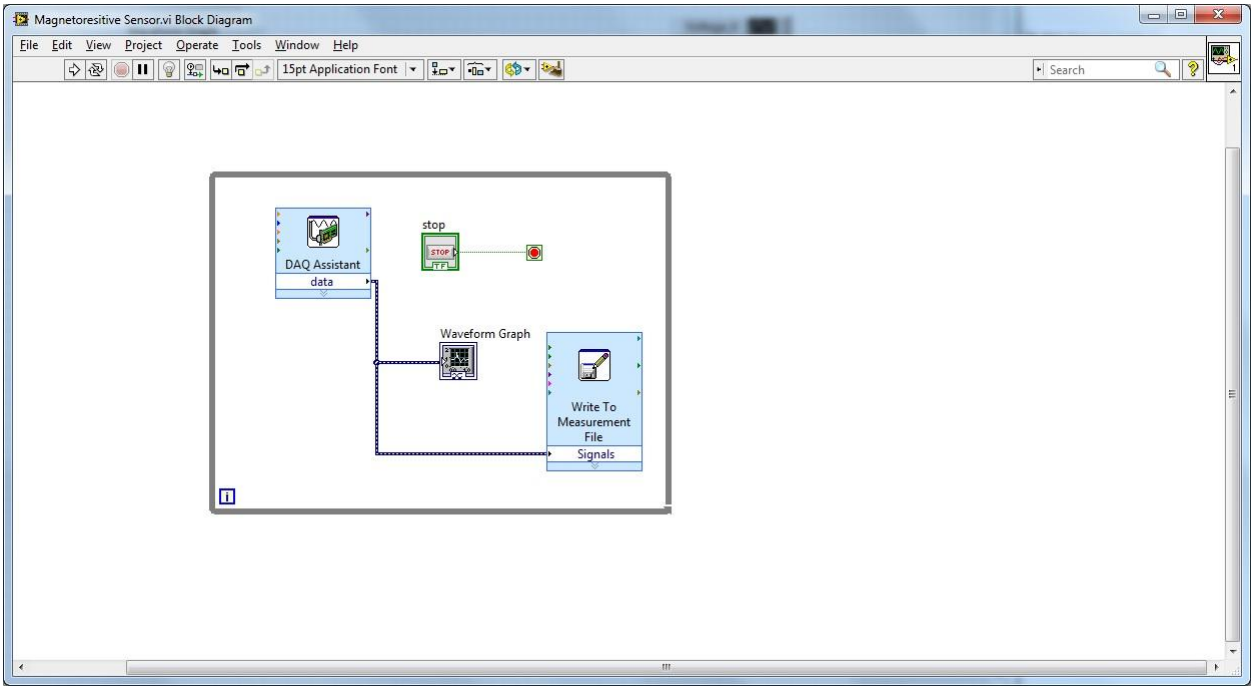

Figure 6: LabVIEW Block Diagram for Magnetometer setup

The settings for the DAQ Assistant are four analog input channels ai0 & ai4, ai1 & ai5 configured for voltage measurement and connected differentially with the N samples rate selected. The "Samples to Read" and "Rate [Hz]" options are set to 1k, but can be altered in such way that LabVIEW can output better looking graphs.

Experimental Results:

After setting up the circuit and the LabVIEW DAQ graphical interface, the user can collect the data from the magnetometer by placing it on an axis that it can spin/rotate uniformly to obtain a characteristic representation of the magnetic field during rotation. The most convenient method is using a spinning office chair in the laboratory to observe its behavior; slow-motion motors would require a hole or fastener in the breadboard (not practical) to accurately simulate rotation around an axis. The y-axis can be expressed as magnetoresistance versus the strength of the magnetic field emitted from internal barber pole structure of the sensor.

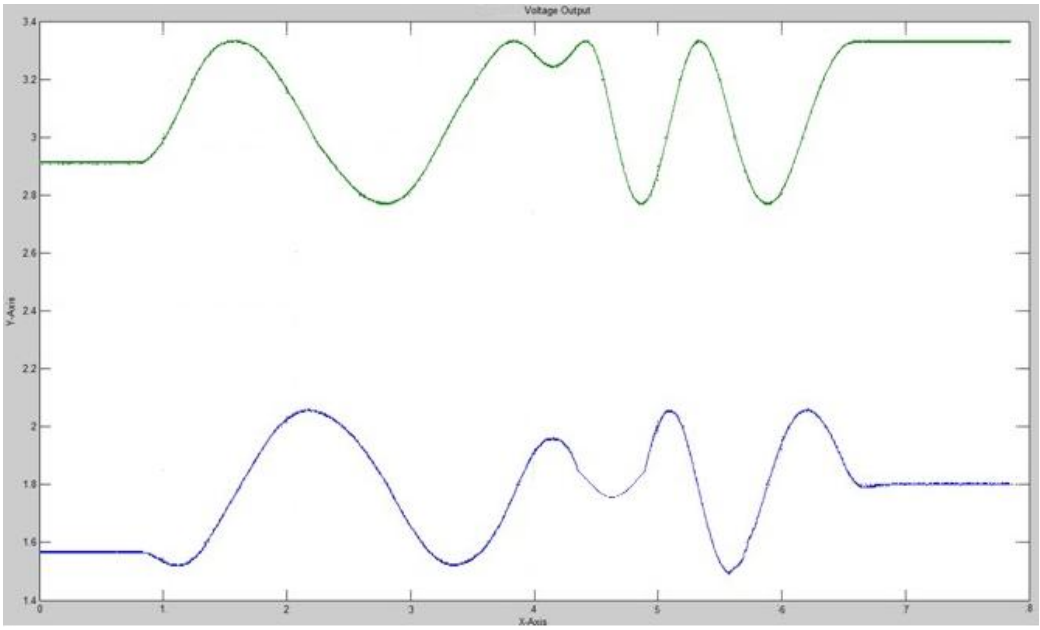

Figure 7: Sinusoid voltage output of the magnetometer axes; both waves appear to be out of phase by 90 degrees.

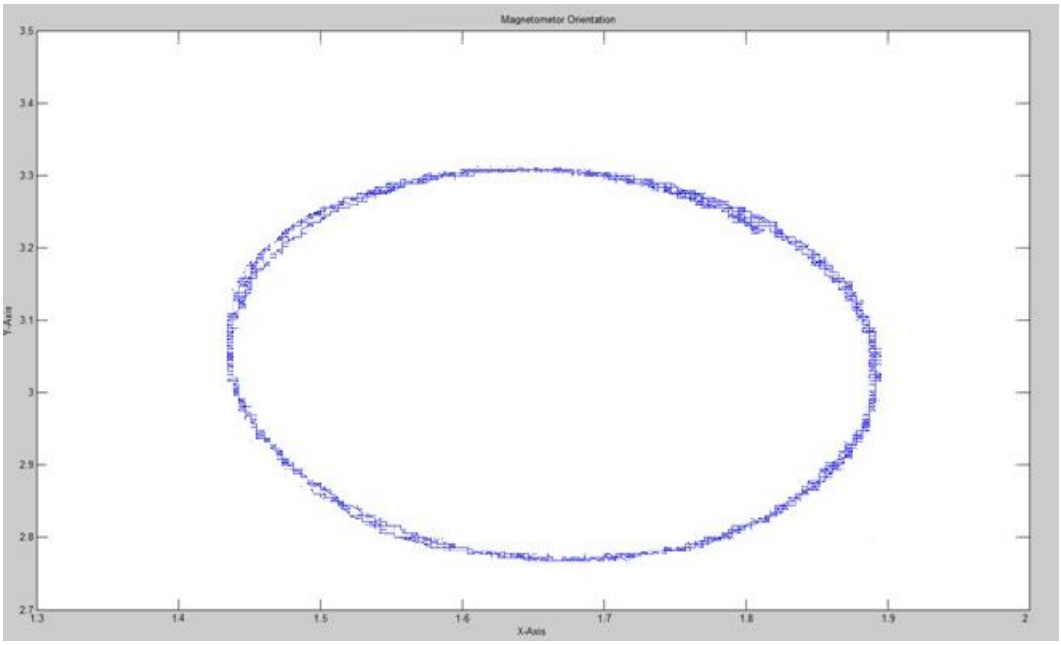

Figure 8: Voltage outputs of Die A and B plotted against each other forming the unique ellipsoid graph

After rotating the magnetometer by a few full turns, the waveform cycles three times at show some 90 degree phase shift (perpendicular) that one could map to the compass directions NWSE.

Figure 9: A lodestone magnet I bought on the trip to Utah to use to test the S/R straps of the HMC1022 sensor in saturating and distorting the magnetic fields.

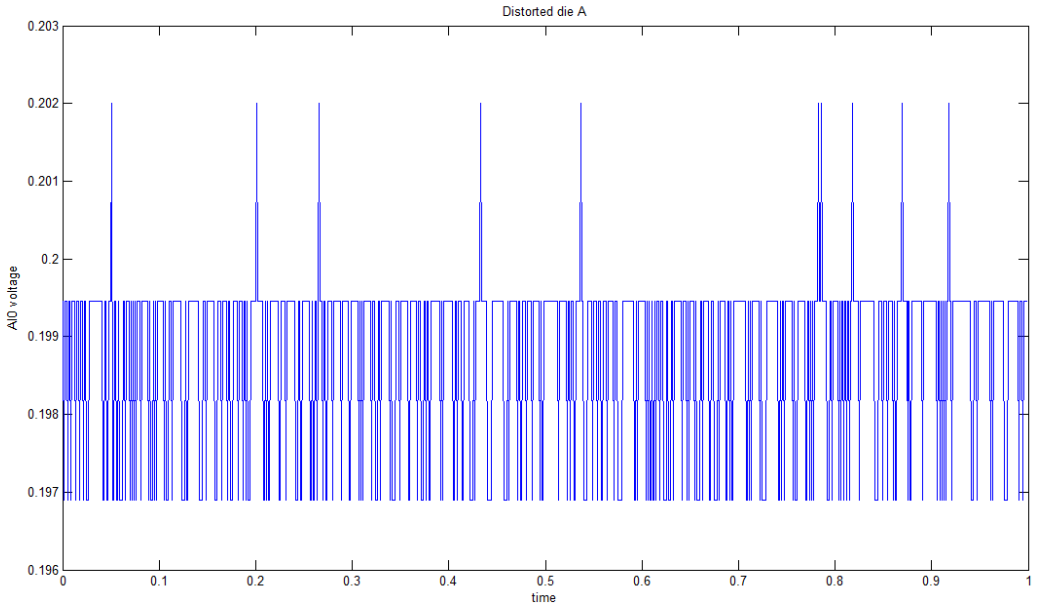

Figure 10: die A x-axis under with saturated magnetic field exposed to lodestone magnet.

Exposing the natural magnet to the magnetometer sensor seems to greatly affect the representation of the sine waves below. The waveforms have clipped tops and resemble rectangular pulse trains, but are recognizably distorted sine waves. I was not able to reset the

waveforms back to their original, clean waveform behavior after checking circuit connections 12 times, replacing the magnetometer device (by exposing it to the magnet and using the set/reset circuit), and using different analog inputs of the DAQ device. The supposed egg shaped waveform appears to have random magnetic domain orientations, though it still recognizable as ellipsoid mapping. The waveform oscillates between two values, though it could be the effects of the unsteady magnetometer sensor output.

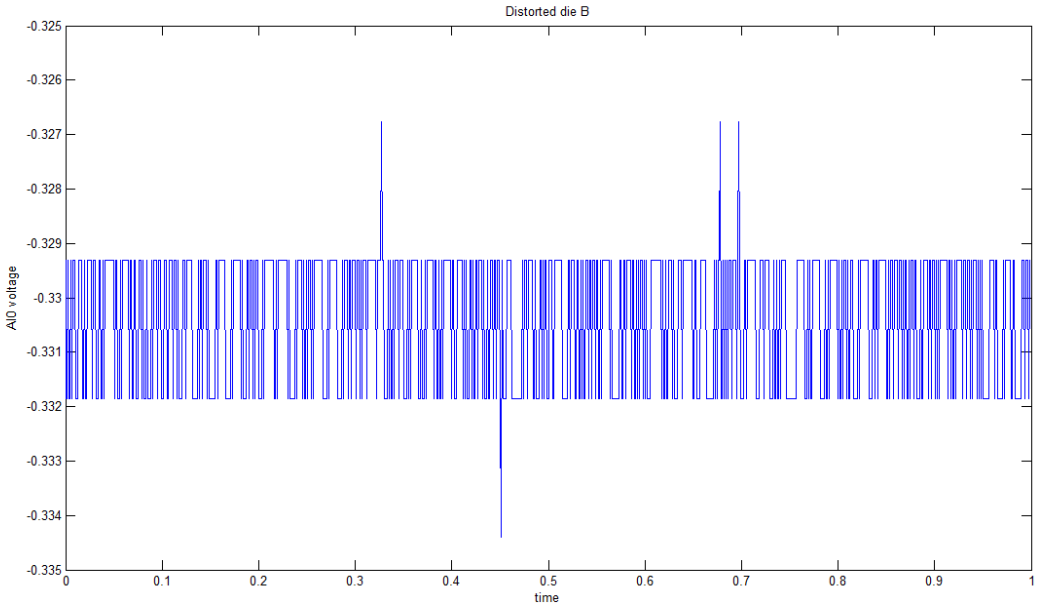

Figure 11: die B y-axis under with saturated magnetic field exposed to lodestone magnet

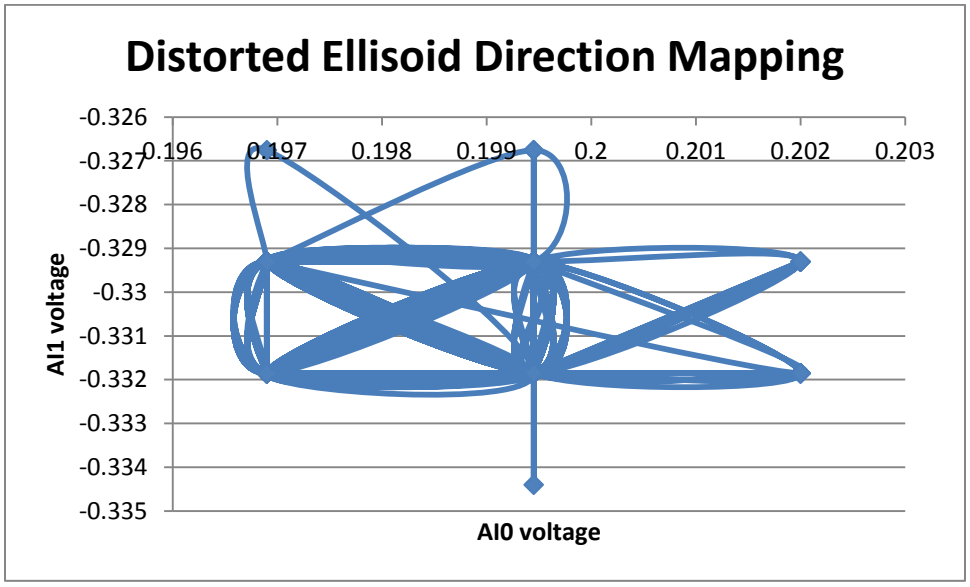

Figure 12: The “mysterious” rounded ellipsoid mapping of analog inputs from the x and y axis (was not able to import to MATLAB)

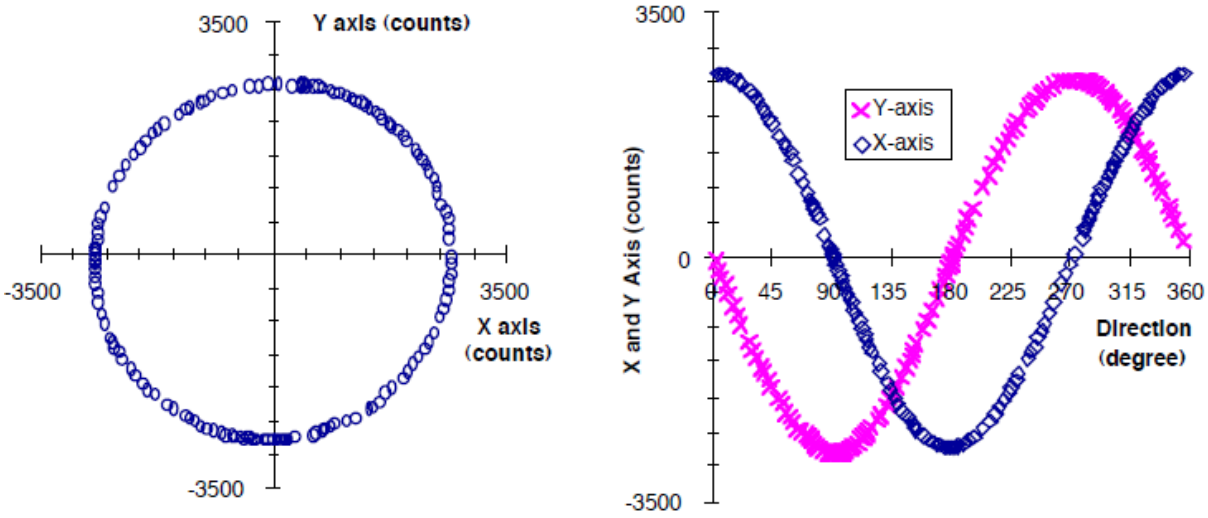

Figure 13: Expected (Corrected) 2-axis magnetometer readings for 360° rotation in a level plane with tilt and ferrous distortion compensation. Notice the 90 degree phase shift of the second, which allows for directional mapping.

Conclusion:

Magnetoresistive sensors provide a great, solid-state solution for compass navigation with their high sensitivity, repeatability, and portability, resulting in a high accuracy, integrated magnetic sensor. The next steps to follow in carrying out the experiment would be tilt and ferrous distortion compensation, as seen by the ellipsoid generated by the LabVIEW results. The general ellipsoid magnetic field shape is acceptable enough for a gentle introduction to observing the behavior of the magnetic field affected by elemental factors. Furthermore, a cheap microcontroller can be used to interface the serial bus output for azimuth angle computation. If I had done the experiment at the same time with my classmates, I would have received more help in understanding the magnetoresistive sensor properties since some learning is best done by collaborative explanation and reasoning.

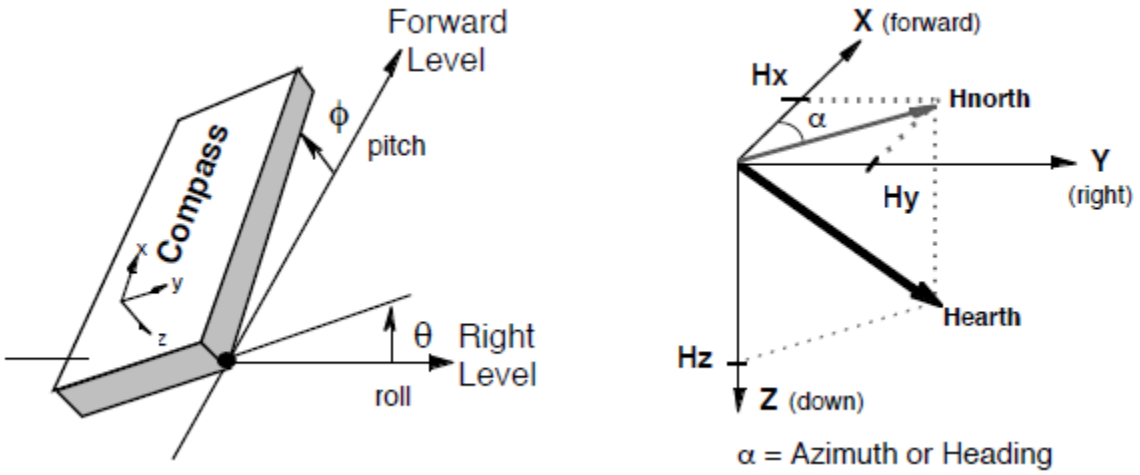

$$
\begin{aligned}
&\text{Azimuth } (x=0,\ y<0) && = 90.0 && (3)\\
&\text{Azimuth } (x=0,\ y>0) && = 270.0\\
&\text{Azimuth } (x<0) && = 180 - [\arctan(y/x)]*180/\pi\\
&\text{Azimuth } (x>0,\ y<0) && = - [\arctan(y/x)]*180/\pi\\
&\text{Azimuth } (x>0,\ y>0) && = 360 - [\arctan(y/x)]*180/\pi
\end{aligned}
$$

Figure 14: Equations describing continuous azimuth angles from 0-360 degrees in the forward direction in relation to magnetic north (H_{NORTH})

Improvements:

Honeywell provides additional detail to the problem of sensor bridge offset in AN212. It follows up on the laboratory about non-exact nature of internally-matched Wheatstone bridge resistor pairs, concerning the full accuracy of the sensor in precise applications around a few milli-gauss range of measuring the Earth's magnetic field. The details are provided in the reference [1] below; a summary of the topic would not adequate to explain the details as well as the application note features. The design could accommodate for tilt compensation using a tilt sensor for better compass operation from using a three magnetic axis magnetoresistive sensor, since the sensor we tested was placed on a level surface and then spun. Tilt compensation for 3D system complicates finding the azimuth, or heading direction as the compass does not stay horizontal to the earth's surface. Inclinometers can provide the solution to correct compass tilt in determining roll (rotation around X) and pitch (rotation around Y) angles.

The data acquisition devices could have better resolution to view sampled waveforms more accurately and cleanly. Some alternate, low-budget DAQ devices the university could invest with better resolution would be the NI-6009 DAQ or the myDAQ device. A third-party, National Instruments supported DAQ device called SensorDAQ is provided on the link below through the company Vernier.

http://www.vernier.com/products/interfaces/sdaq/

http://www.studica.com/National-Instruments-students-ni-labview-mydaq/ni-mydaq.html

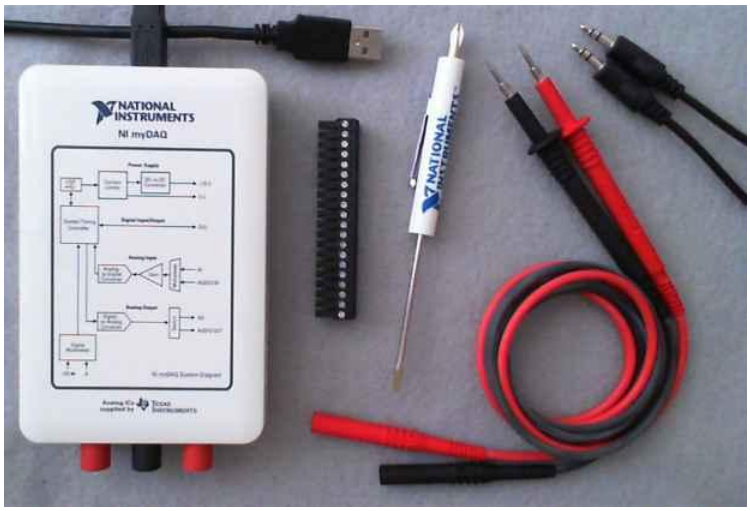

The magnetoresistive sensor can use utilize a simple calibration procedure to determine the offset and scale factor values based on the magnetometer readings from the x-axis and y-axis dies generated from the data acquisition device.

- Mount the compass in the car and drive the car in a circle on a horizontal surface.
- Find the maximum and minimum values of the X and Y magnetic readings.
- Using these four values determine the X and Y scale factors (Xsf, Ysf) and the zero offset values (Xoff, Yoff).

$$Xsf = 1 \text{ or } (Ymax - Ymin) / (Xmax - Xmin) \quad (6)$$
whichever is greater

$$Ysf = 1 \text{ or } (Xmax - Xmin) / (Ymax - Ymin)$$
whichever is greater

$$Xoff = [(Xmax - Xmin)/2 - Xmax] * Xsf \quad (7)$$

$$Yoff = [(Ymax - Ymin)/2 - Ymax] * Ysf$$

The following example will show how the compensation values are determined. A compass is mounted in a car that has traveled a circle in a vacant parking lot. The magnetic X and Y counts (15,000 counts=1 gauss) from the magnetometer are scanned and the minimum and maximum readings are:

$$Xmin = -3298 \quad Xmax = 2338$$

$$Ymin = -3147 \quad Ymax = 1763$$

Set the X scale factor (Xsf) to one since (Ymax - Ymin)/(Xmax - Xmin)< 1, according to equation (5). Next, determine the Y scale factor (Ysf) by dividing the X reading span by the Y reading span.

$$Xsf = 1$$

$$Ysf = (Xmax - Xmin) / (Ymax - Ymin) = 1.15$$

Calculate the offset correction values by taking one-half the difference of the max. minus min. readings and apply the scale factors, Xsf and Ysf.

$$Xoff = [(Xmax - Xmin)/2 - Xmax] * Xsf = 480$$

$$Yoff = [(Ymax - Ymin)/2 - Ymax] * Ysf = 795$$

Store these values and apply them to every tilt compensated reading—X_H and Y_H. The Xvalue and Yvalue numbers used in the azimuth calculations, equations (3), to determine compass heading are:

$$Xvalue = XH + 480$$

$$Yvalue = 1.15 * Y_H + 795$$

Figure 15: Calibration algorithm procedures [4]

References:

Petersen's list of application notes from Zetex:
http://classes.soe.ucsc.edu/cmpe167/Winter13/

Honeywell's HMC1022 Application Notes Website: Search Tool: HMC1022
http://honeywell.com/Pages/Search.aspx?k=HMC1022

Specific Application Notes:

[1] http://www51.honeywell.com/aero/common/documents/myaerospacecatalog-documents/Defense_Brochures-documents/Magnetic__Literature_Application_notes-documents/AN212_Handling_of_Sensor_Bridge_Offset.pdf

[2] http://www51.honeywell.com/aero/common/documents/myaerospacecatalog-documents/Defense_Brochures-documents/Magnetic__Literature_Application_notes-documents/AN213_Set_Reset_Function_of_Magnetic_Sensors.pdf

[3] http://www51.honeywell.com/aero/common/documents/myaerospacecatalog-documents/Defense_Brochures-documents/Magnetic__Literature_Application_notes-documents/AN218_Vehicle_Detection_Using_AMR_Sensors.pdf

[4] http://www.newsmans-blog.de/redmine/files/110819154322_Compass_tilt_compensation.pdf